

Cooling rates and crystallization dynamics of shallow level pegmatite-aplite dikes, San Diego County, California

KAREN L. WEBBER,^{1,*} WILLIAM B. SIMMONS,¹ ALEXANDER U. FALSTER,¹ AND EUGENE E. FOORD^{2,†}

¹Department of Geology and Geophysics, University of New Orleans, New Orleans, Louisiana 70148, U.S.A.

²U.S. Geological Survey, Denver Federal Center, Denver, Colorado 80225, U.S.A.

ABSTRACT

Pegmatites of the Pala and Mesa Grande Pegmatite Districts, San Diego County, California are typically thin, sheet-like composite pegmatite-aplite dikes. Aplitic portions of many dikes display pronounced mineralogical layering referred to as “line rock,” characterized by fine-grained, garnet-rich bands alternating with albite- and quartz-rich bands. Thermal modeling was performed for four dikes in San Diego County including the 1 m thick Himalaya dike, the 2 m thick Mission dike, the 8 m thick George Ashley dike, and the 25 m thick Stewart dike. Calculations were based on conductive cooling equations accounting for latent heat of crystallization, a melt emplacement temperature of 650 °C into 150 °C fractured, gabbroic country rock at a depth of 5 km, and an estimated 3 wt% initial H₂O content in the melt. Cooling to <550 °C at the center of each dike occurred in ~9 years for the Stewart dike, ~340 days for the George Ashley dike, ~22 days for the Mission dike, and ~5 days for the Himalaya dike. Based on these calculations, growth rates for large pegmatitic minerals such as the 10 cm long Himalaya hanging wall tourmaline crystals may have been on the order of 10⁻⁵ cm/s. Crystal size distribution (CSD) studies of garnet from layered aplites suggest growth rates of about 10⁻⁶ cm/s. These results indicate that the dikes cooled and crystallized rapidly, with variable nucleation rates but high overall crystal-growth rates. Initial high nucleation rates coincident with emplacement and strong undercooling can account for the millimeter-size aplite grains. Lower nucleation rates coupled with high growth rates can explain the decimeter-size minerals in the hanging walls, cores, and miarolitic cavities of the pegmatites. The presence of tourmaline and/or lepidolite throughout these dikes suggests that although the melts were initially H₂O-undersaturated, high melt concentrations of incompatible (or fluxing) components such as B, F, and Li (±H₂O), aided in the development of large pegmatitic crystals that grew rapidly in the short times suggested by the conductive cooling models.

INTRODUCTION

Pegmatites are characterized by crystals of very large size. Many people have assumed that these crystals attained their size as a result of long periods of growth from slowly cooled magmas. Some pegmatites, however, are intimately associated with fine-grained aplites (commonly along the footwall portions of the dikes), for which grain sizes are suggestive of much faster cooling, nucleation, and crystal growth. The contrast in crystal size between the genetically related coarse-grained pegmatite and fine-grained aplite remains one of the intriguing enigmas with respect to the genesis of these pegmatite-aplite dikes. Many of the pegmatites in San Diego County have layered aplites and were first described in detail by Jahns and Tuttle (1963). Layered portions of pegmatite-aplite dikes are locally known as “line rock.”

This paper presents a conductive cooling-crystallization model for four composite pegmatite-aplite dikes in San Diego County, California: the George Ashley, Stewart, and Mission dikes in the Pala Pegmatite District and the Himalaya dike in the Mesa Grande Pegmatite District. The aplitic portions of all

except the Stewart display well-developed rhythmic layering of alternating garnet-rich and garnet-poor layers.

Typically, variations in grain size throughout a dike or sill are small (2–3 orders of magnitude), and grain size generally increases uniformly from dike margin to center (Cashman 1990). In contrast, most pegmatite-aplite dikes display changes in crystal size from <0.1 mm in aplites, to >10 cm for crystals in the hanging wall, core zone, and pockets. In addition, the grain size does not always increase consistently from the margins to the core. Pegmatite-aplite dikes typically have a fine-grained footwall, coarse-grained hanging wall, and a core zone with miarolitic cavities. However, individual dikes display a wide range in grain size. Footwall aplites can be layered or nonlayered, layered aplites can alternate with pegmatite, and aplites can occur in an irregular distribution throughout the footwall. Clearly, changes in grain size of ~5 orders of magnitude, and an irregular distribution of grain size with respect to the dike margins and centers, indicate that crystallization parameters such as nucleation and growth rates are not consistent during the crystallization history of pegmatite-aplite dikes. The role of both undercooling and volatiles is critical to the development of textural features that characterize pegmatite-aplite dikes. To explain the textures characteristic of pegmatites,

*E-mail: kwebber@uno.edu

†Deceased: January 8, 1998.

strong undercooling is required. Although pegmatitic melts might not be water saturated upon emplacement (London et al. 1989; London 1992), they must become saturated at some point during their crystallization in order to form miarolitic cavities. The San Diego County pegmatites had high enough concentrations of B, Li, F, and Be that tourmaline, spodumene, lepidolite, and beryl were able to form.

Kleck (1996) proposed that the layering in the George Ashley Block, a landslide block from this dike, could be explained by the gravitational settling of garnet and albite from the melt, and that many of the textural features that characterize the line rock, such as offsets in the layers, formed as a result of soft sediment deformation of a crystal-liquid mush. Webber et al. (1997) investigated the line rock associated with the George Ashley dike and suggested that the high melt viscosity and short dike cooling time would have precluded any significant amount of settling in the dike prior to solidification. They proposed that the layering was the result of a mechanism of diffusion-controlled oscillatory nucleation and crystallization.

GEOLOGIC SETTING

The George Ashley, Mission, and Stewart dikes are located in the Pala Pegmatite District in northwestern San Diego County, California (Fig. 1). At least 400 pegmatite dikes occur in this district, which covers an area of about 22 km² (Jahns and Wright 1951). The Pala district is famous for many gem-bearing pegmatites that have produced gem quality tourmaline, spodumene, and beryl (morganite), as well as commercial quantities of lepidolite. The pegmatites are situated in the western portion of the Peninsular Ranges geologic province, which roughly parallels the Pacific coast. The Pala pegmatites are very uniform in shape and attitude, being chiefly subhorizontal tabular dikes, trending within a few degrees of north, and having average dips of 20° west. Almost without exception, the pegmatites are en-

closed in host rocks of gabbroic composition. This uniformity in shape and attitude is consistent with pegmatite emplacement along well-developed fracture sets in the older gabbro, and most irregularities that do occur in the shapes of dikes, i.e., branching or bulging, can be attributed to irregularities in the pattern of fractures. The fractures bear no systematic relation to the shapes or attitudes of the Peninsular Ranges plutons, as they cut across contacts between crystalline rocks of different composition and are very uniform in orientation, trending north and dipping gently to moderately west (Jahns and Wright 1951). The fractures are thought to have resulted from regional cooling and contraction within the batholith as a whole, and fracture development postdated the main period of batholith emplacement (Jahns 1979). Contacts between pegmatites and host rock are generally sharp, and host rock alteration adjacent to pegmatite bodies is minor (Foord et al. 1986).

San Diego County pegmatites are the youngest rocks in the western portion of the Peninsular Ranges batholith (Foord et al. 1991). No direct source for the pegmatites has been located and they were preferentially emplaced into gabbro and norite of the 118–120 Ma San Marcos Gabbro. Pegmatites that have been dated radiometrically yield ⁴⁰Ar/³⁹Ar emplacement ages of 99–100 Ma (Foord et al. 1991). The age of the San Marcos Gabbro adjacent to pegmatites, as determined from both biotite and hornblende ⁴⁰Ar/³⁹Ar geochronology, was reset to the time of pegmatite emplacement (Snee and Foord 1991). However, samples collected from the spatially associated Woodson Mountain Granodiorite at distances up to 15 km away from the pegmatites have not been affected by pegmatite intrusion. According to Foord et al. (1991), this granodiorite was emplaced prior to 113 Ma (hornblende age) and had cooled below 300 °C (biotite Ar-retention temperature) by 107 Ma (biotite apparent age), and below 150 °C (microcline Ar-retention temperature) by 104 Ma (microcline apparent age) prior to pegmatite emplacement. This temperature of 150 °C is consistent with that obtained using a geothermal gradient of 30 °C/km for pegmatite melts emplaced at a depth of 5 km.

The Stewart pegmatite is located on the eastern slope of Queen Mountain. It can be traced laterally for almost 1 km and is up to 25 m wide. The pegmatite is complexly zoned with a quartz-spodumene core, several intermediate zones, a thick hanging wall zone of coarse-grained graphic granite, and a footwall that is comprised in part of a non-layered, fine-grained aplite. Two large pods of lepidolite located beneath the quartz-spodumene core were mined extensively in the 1920s (Jahns and Wright 1951). The Stewart pegmatite currently is being mined for gem tourmaline.

The Mission dike is located on the south slope of Queen Mountain. The dike has an average thickness of 2 m, trends north, and dips 25° west. The pegmatite-host gabbro contacts are sharp and both are cut in several places by faults having small displacements (Jahns and Wright 1951). The structure of the dike is simple and consists of a hanging wall composed of coarse-grained graphic granite, a central zone of albite-quartz-perthite-muscovite rock, and an extensive, well-developed footwall consisting primarily of garnet-rich line rock. Some lepidolite and gem quality tourmaline have been recovered in the past.

The best exposures of the George Ashley dike are as large

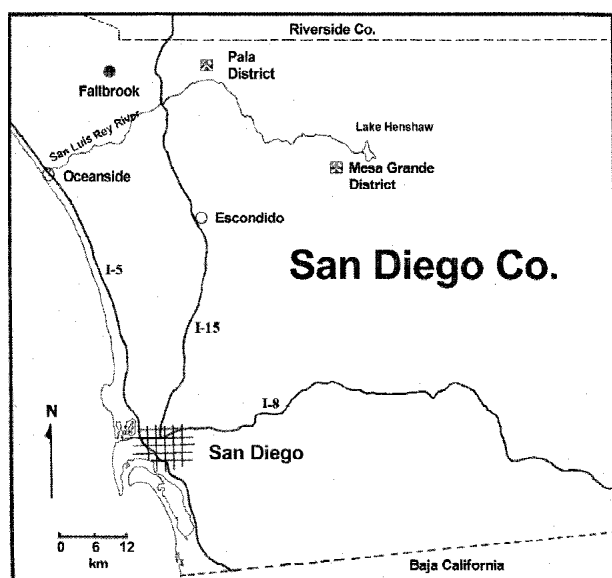


FIGURE 1. Location map for the Pala and Mesa Grande Pegmatite districts in San Diego County, California.

landslide blocks located on the eastern slope of Hiriart Mountain. The blocks that came from the George Ashley dike are associated with the Vanderburg-Katerina dike group (Jahns and Wright 1951). The George Ashley dike is tabular with an exposed thickness of 8 m and a width of 15 m. It is characterized by a spectacular footwall quartz-albite aplite that is rhythmically layered with garnet-rich bands (Fig. 2a). According to Jahns and Wright (1951), garnet-rich line rock is more prevalent in the pegmatites on Hiriart Mountain than elsewhere in the Pala District. The lower 245 cm of the dike are comprised of granular pegmatite with quartz, microcline, albite, and muscovite. The distinctly layered line rock begins 245 cm above the base and extends upward for 70 cm. It is characterized by garnet-enriched (almandine-spessartine solid-solution) layers alternating with layers enriched in albite, quartz, and muscovite with small amounts of microcline, biotite, and tourmaline. Above the line rock region is a core zone of coarse quartz and perthitic microcline (Fig. 2b). Tourmaline crystals up to 15 cm in length occur in sparse pockets associated with the core. Overlying the core zone is granular pegmatite with scattered garnet



FIGURE 2. (a) Well-developed layered aplite (line-rock) in the footwall of the George Ashley dike. The dark-colored layers are enriched in garnet and the light-colored layers in albite and quartz. Microcline megacrysts are in the center of some of the nested loops. (b) The transition from line rock to the overlying pocket zone in the George Ashley dike. This is one of the large landslide blocks, up is to the left.

and blocky graphic intergrowths of microcline and quartz. This grades upward into finer-grained granular pegmatite that lacks graphic intergrowths of quartz and potassium feldspar.

The Himalaya dike, one of the most prolific producers of gem tourmaline in San Diego County, is located in the Mesa Grande Pegmatite District (Fig. 1). Approximately 90 pegmatites occur within this district in an area of several square kilometers (Foord et al. 1991). Like the pegmatites in the Pala district, the majority of the pegmatites in the Mesa Grande district are tabular in shape, strike north to northwest, dip slightly to the west or southwest, and are hosted by gabbronorite. The Himalaya dike system consists of two subparallel pegmatite-aplite dikes ranging in combined thickness from <0.5 m to 2 m, along with several additional thin branches. The two main dikes can be as much as 3 to 10 m apart, but converge southward where they are in direct contact for a distance of >18 m (Foord 1977). The Himalaya dike system can be traced continuously for a distance of 915 m along strike (Fisher et al. 1998). The upper of the two dikes is thinner and has been the principal source of gem quality specimens (Fig. 3). Jahns (1979) referred to the upper dike as the "Himalaya Dike." Each dike consists of a layered to nonlayered footwall aplite zone, a central pocket zone, and a hanging wall graphic pegmatite zone (Fig. 4); considerable along-strike variations in the thickness of each zone have been noted (Foord 1976). Field relations indicate that the upper dike intruded the lower dike after crystallization of a portion of the aplite zone in the latter (Foord 1976). The upper Himalaya dike has been mined for gem quality tourmaline at both the Himalaya Mine and along strike to the south at the San Diego Mine. The Himalaya samples used for the crystal size distribution study came from the upper dike exposed in the San Diego Mine. At this location, the dike is 1 m thick and can be divided into three zones. The lower third consists of graphic granite and pegmatite, the middle third consists of layered aplite and pegmatitic aplite (a rock with an aplitic texture that contains tapered potassium feldspar megacrysts in addition), and the upper section has a pocket zone that in turn is overlain by graphic and massive pegmatite zones (Foord 1976).



FIGURE 3. Photograph of the upper Himalaya dike exposed in the Himalaya Mine. Large schorl crystals, some over 10 cm in length, can be seen growing out in a comb structure from the pegmatite hanging wall-country rock contact.

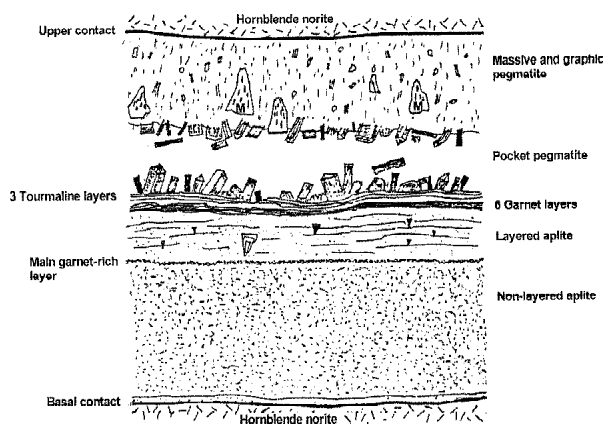


FIGURE 4. Schematic diagram of the lower Himalaya dike as exposed in the San Diego Mine. Thickness of the dike here is 135 cm. The tapered crystals (labeled "M") in both the hanging wall and footwall are potassium feldspar (microcline) megacrysts.

CHARACTERIZATION OF THE GEORGE ASHLEY DIKE

The George Ashley dike was characterized chemically and mineralogically in Webber et al. (1997), and parameters such as density, viscosity, pressure, and depth of emplacement were determined. These data are summarized here, as these same parameters were used to establish the cooling and crystallization models for the Stewart, Mission, and Himalaya dikes.

Based on major and trace-element analysis, the George Ashley samples can be characterized as peraluminous (average $A/CNK = 1.23$). Overall, no consistent fractionation trends are seen from the bottom to the top of the George Ashley dike. There is no evidence that the melt was water-saturated upon emplacement, and saturation was likely only achieved in the final stages of core crystallization with the development of a few small pockets. Overall B concentrations are low, but increase inward from both the top and bottom of the pegmatite toward the core zone. Fluorine abundances in muscovite also increase inward from both the top and bottom of the pegmatite. No metasomatic alteration of the adjacent country rock, which should have been produced by a vapor phase escaping from the crystallizing pegmatite, is observed. Thus, a melt H_2O content of 3 wt% was chosen for calculation purposes, which would permit crystallization of at least 75% of the dike before vapor saturation occurred. The estimated temperature of emplacement for the melt was 650 °C based on mineral equilibria of the assemblage quartz, plagioclase, potassium feldspar, muscovite, and garnet (Huang and Wyllie 1981). The average composition of the George Ashley melt falls close to the 1.5 kbar H_2O saturated minimum in the haplogranite system, which corresponds to an emplacement depth of ~5 km into previously fractured, brittle country rock. The density of the magma, calculated by averaging all 15 whole-rock analyses, is 2.31 g/cm³. Viscosity, η , calculated using the empirical model of Baker (1996) for 3.0 wt% H_2O is 10^{6.2} Pa·s.

CONDUCTIVE COOLING MODEL

To constrain a realistic cooling model, many parameters related to the magma and its intrusion need to be evaluated

(temperature and depth of emplacement, thermal diffusivity, latent heat of crystallization, temperature interval of crystallization, and intrusion size). Thermal modeling also requires knowledge about the initial temperature, thermal diffusivity, and geothermal gradient of the host rock (Jaeger 1968). Additionally, one must evaluate whether conductive or convective processes were acting upon the magma body during crystallization. As discussed in Webber et al. (1997), the dominant mechanism of heat transport in the thin, shallow George Ashley dike was conduction. We have modeled cooling in the Stewart, Mission, and Himalaya dikes with the same conductive cooling model, which is also appropriate for these shallow dikes. As previously discussed we used a melt emplacement temperature of 650 °C into 150 °C brittle country rock for the thermal modeling. The temperature interval of magmatic crystallization thus began at 650 °C and, for haplogranite melts of this composition, crystallization should have been essentially completed by the time the magma cooled to ~550 °C.

The simplifying assumption that thermal diffusivity was the same for both magma and country rock was used for the cooling models. Thermal diffusivity can be defined as:

$$= K / C_p \quad (1)$$

where α is thermal diffusivity in cm²/s, K is the coefficient of thermal conductivity measured in cal/cm·s·°C, ρ is density in g/cm³, and C_p is heat capacity in cal/g·°C. Heat capacity is defined by:

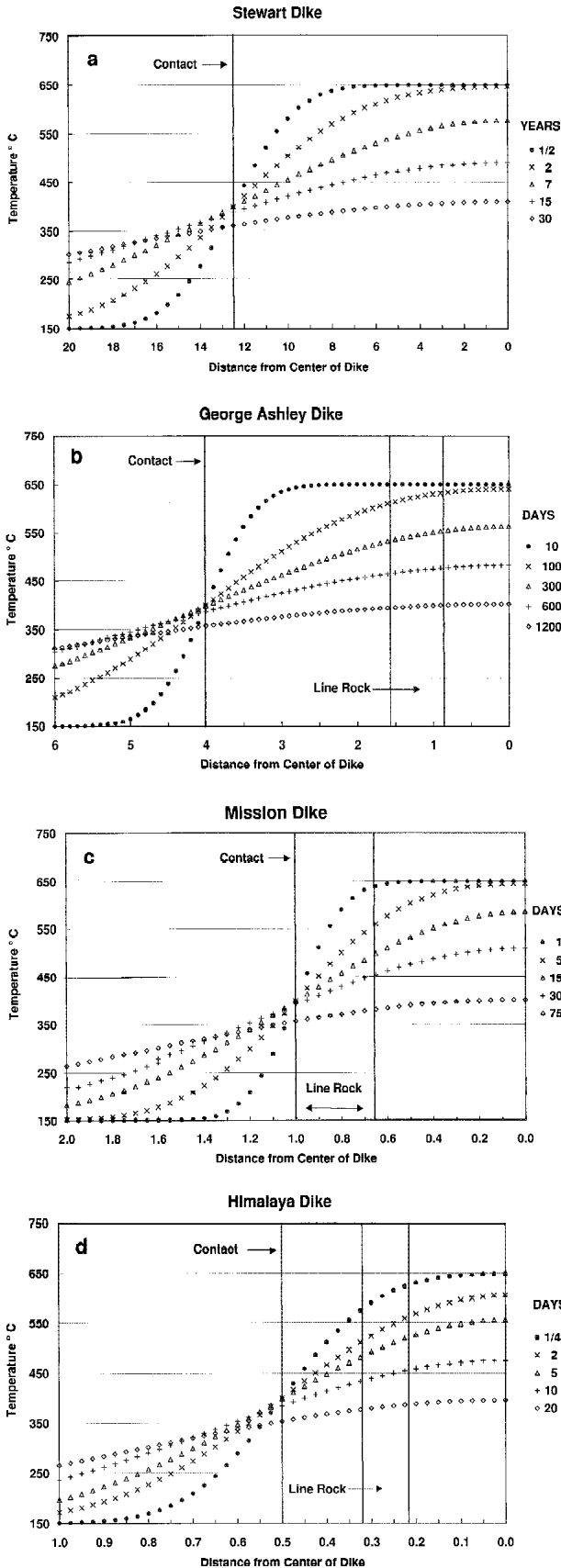
$$C_p = q / T \quad (2)$$

in which q is the amount of heat that must be added or removed to raise or lower the temperature of one gram of matter by one degree celsius. Heat of crystallization, q_c , is the heat liberated by the crystallization of one gram of melt that is already at the temperature where the liquid and solid coexist. For most rocks C_p is ~0.3 cal/g·°C, whereas typical values for q_c are ~60–100 cal/g (McBirney 1993). This amounts to roughly the same amount of heat in the crystallization of a melt as in raising the temperature of the melt by 200–300 °C, which will reduce the rate of cooling of the magma as it passes through the crystallization interval. The heat of crystallization q_c , released during crystallization through a temperature interval $T_1 - T_2$, can be accommodated by adding the proportional heat per degree to the heat capacity to obtain an effective heat capacity, h (Jaeger 1968):

$$h = C_p + \frac{q_c}{(T_1 - T_2)} \quad (3)$$

This expression can be substituted for C_p in Equation 2 to obtain an appropriate value that accounts for the heat of crystallization.

Using values of 0.3 cal/g·°C for C_p , 75 cal/g for q_c (McBirney 1993), and a temperature interval ($T_1 - T_2$) of 100 °C (from 650 to 550 °C), the effective heat capacity (h) is 1.05 cal/g·°C. Then, using a thermal conductivity (K) of 4×10^{-3} cal/cm·s·°C and the George Ashley calculated magma density of 2.31 g/cm³, results in a thermal diffusivity (α) of 1.66×10^{-7} m²/s. The thermal diffusivity obtained by not taking latent heat of crystallization into account, and using the same magma density, heat capacity, and thermal conductivity, is 5.80×10^{-7} m²/s.



The conduction equation for a sheet of thickness $2a$ (Jaeger 1968) assuming the same thermal diffusivity, α , for both magma and country rock is the following:

$$T / T_0 = \frac{1}{2} \operatorname{erf} \frac{x/a + 1}{2\sqrt{t/a^2}} - \operatorname{erf} \frac{x/a - 1}{2\sqrt{t/a^2}} \quad (4)$$

where

$$\operatorname{erf}(y) = \frac{2}{\sqrt{\pi}} \int_0^y e^{-u^2} du;$$

T is the temperature at time t (in seconds) at distance x (in meters) from the mid-plane of the sheet minus the country rock temperature; $T = T(x, t) - T_{cr}$; and $T_0 = T_m - T_{cr}$ where T_m is equal to the initial magma temperature and T_{cr} is equal to the country rock temperature. For ease of calculation, the erf function can be approximated (Philpotts 1990) by:

$$\operatorname{erf}(y) = 1 - (a_1 - a_2 y^2 + a_3 y^3) \exp[-(y^2)] \quad (5)$$

where

$$= 1/(1 + 0.47047y); a_1 = 0.34802; a_2 = -0.09587; \text{ and } a_3 = 0.74785.$$

The cooling history for each dike was modeled in two ways. The first model assumed no latent heat of crystallization during the crystallization of the dike and used a thermal diffusivity of $5.80 \times 10^{-7} \text{ m}^2/\text{s}$. Cooling to $<550^\circ\text{C}$ at the center of each dike occurred in ~ 1000 days for the 25 m thick Stewart dike, 100 days for the 8 m thick George Ashley dike, 6 days for the 2 m thick Mission dike, and 1.5 days for the 1 m thick Himalaya dike. The second model, which accounts for latent heat of crystallization by using a modified thermal diffusivity value of $1.66 \times 10^{-7} \text{ m}^2/\text{s}$ slows the rate of cooling such that cooling to $<550^\circ\text{C}$ took place in ~ 9 years for the Stewart dike (Fig. 5a), 340 days for the George Ashley dike (Fig. 5b), 22 days for the Mission dike (Fig. 5c), and 5 days for the Himalaya dike (Fig. 5d). The cooling rates obtained by accounting for latent heat of crystallization will be used in subsequent discussions on crystallization dynamics.

GARNET CRYSTAL SIZE DISTRIBUTION

Theory

The theory of Crystal Size Distribution (CSD) was developed initially by chemical engineers (Randolph and Larson 1971) for evaluating kinetics of crystallization, i.e., growth and nucleation rates, of industrial compounds. CSD is an empirical model of crystal nucleation and growth based on a population balance of crystals in the system. Crystals move into and out of a size range through physical movement in the system and growth into and out of the size range of interest. Marsh (1988) developed the standard CSD theory for geologic systems to

FIGURE 5. Cooling curves for the (a) Stewart, (b) George Ashley, (c) Mission, and (d) Himalaya dikes calculated with latent heat of crystallization. Half-width of the dike is plotted with the dike center at 0 and the position of the contact between the country rock and the dikes shown. Where present, the position of layered aplite (line rock) within the dike is shown.

determine the kinetics of crystallization by examining variations in grain size. Based on grain size information, it is then possible to evaluate nucleation rate, growth rate, and growth time for a population of crystals. Cashman and Marsh (1988) applied CSD theory to rocks from the Makaopuhi lava lake and evaluated growth and nucleation rates for crystals as well as the degree of undercooling. The crystal population density n (number of crystals in a given size class per unit volume) is defined as:

$$n = \frac{N}{L} = \frac{dN}{dL} \quad (6)$$

where L is crystal size and N is equal to the cumulative number of crystals per unit volume less than or equal to L . Assuming that growth rate does not vary with crystal size (Marsh 1988), the population density n of crystals can be related to crystal size L at steady state by:

$$n = n^0 \exp \frac{-L}{G} \quad (7)$$

where n^0 is defined as nucleation density at $L = 0$, G is crystal growth rate, and τ is crystal growth time (residence time). Thus, the dominant crystal size, L_D , is equal to G . A plot of $\ln n$ vs. crystal size L yields a line with a slope of $(-1/G)$ and a y-intercept at $L = 0$ of $\ln n^0$. Following Marsh (1988), nucleation rate J , defined as $dN/dt|_{L=0}$, can be related to growth rate G and nucleation density n^0 through the equation:

$$J = n^0 G \quad (8)$$

Calculations

Garnet crystals in the layered aplites of the George Ashley, Mission, and Himalaya dikes are euhedral and nearly spherical and thus are ideal for CSD studies. The maximum diameter of individual garnet grains in thin sections from each dike were measured using image analysis of backscattered electron (BSE) images (Fig. 6) to yield L values. As the crystal population density n is defined as the number of crystals in a given size class per unit volume, the measured number of crystals per unit area

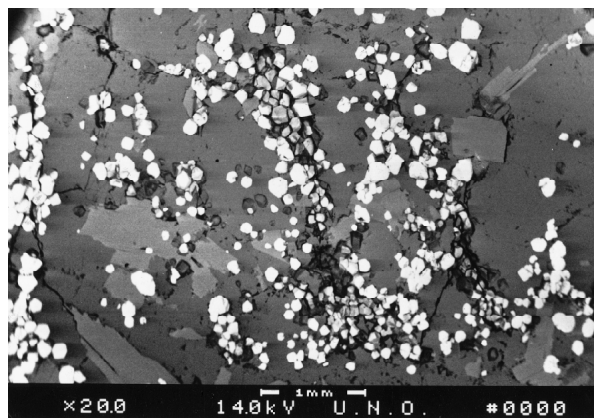


FIGURE 6. Backscattered electron (BSE) image of garnet-rich line-rock from the George Ashley dike. Garnets appear as small bright grains. Bladed and elongated light gray grains are muscovite. Dark gray grains are albite and quartz.

(N_A) was converted to the number of crystals per unit volume (N_V) using the conversion

$$N_V = (N_A)^{1.5} \quad (9)$$

as done by Wager (1961) and Kirkpatrick (1977). Values of n were calculated from measured values of N_V and L of garnets from all three dikes. A cumulative CSD plot of $\ln n$ vs. L for each dike generates a linear trend with a slope of $-1/G$ and an intercept of n^0 , the nucleation density (Fig. 7). A linear regression through the garnet data points was used to calculate the slope and intercept and yields a G value of 5.49×10^{-3} , 2.94×10^{-3} , and 4.34×10^{-3} cm for the George Ashley, Mission, and Himalaya dikes, respectively. The determined n^0 values (given as number of sites per cm^4) are 1.90×10^6 , 6.37×10^7 , and $5.54 \times 10^6/\text{cm}^4$ for the George Ashley, Mission, and Himalaya dikes, respectively.

By substituting the n^0 values determined for each dike into Equation 8, it is then possible to calculate either J or G , if one of the two variables can be determined.

CRYSTALLIZATION PARAMETERS

The textural relationships of minerals in the San Diego County pegmatite-aplite dikes are a reflection of the cooling dynamics and overall nucleation and growth history of the minerals crystallizing from the dikes. In most mafic dikes, crystal size increases only slightly from finer-grained margins to coarser-grained interiors, suggesting that nucleation and growth rates vary only slightly and regularly with time (Cashman and Marsh 1988; Marsh 1988). Such is not the case with the San Diego County pegmatite-aplite dikes, which are characterized by a striking variability in grain size. This heterogeneity suggests variability with respect to crystallization parameters throughout the cooling history of the dikes.

There is abundant textural evidence in both the aplitic and pegmatitic portions of the dikes to support rapid crystal growth rates. The experimental studies of Swanson and Fenn (1986), MacLellan and Trembath (1991), and Fenn (1986) on quartz crystallization in granitic melts demonstrate that skeletal and graphic quartz morphologies reflect rapid crystal growth from a highly undercooled melt. Many quartz grains in the George

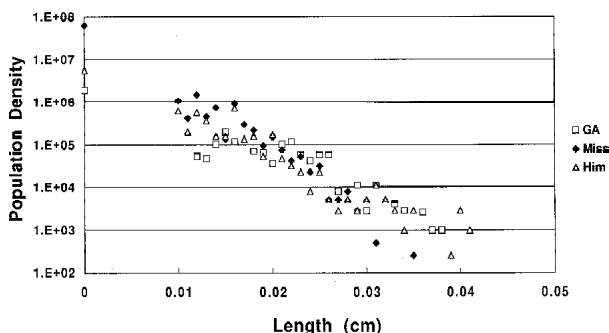


FIGURE 7. Population density (number of sites/ cm^4) vs. length determinations from garnet CSD studies from the George Ashley (open squares), Mission (filled diamonds), and Himalaya (open triangles) dikes. The slope of the best fit line through the data allows determination of the dominant length (G) and the y-intercept of the line yields the population density n^0 , which is shown for each of the dikes.

Ashley layered aplite are skeletal. Grains are elongated parallel to *c* and oriented perpendicular to the layering, and poikilitically enclose albite and garnet (Webber et al. 1997). Graphic intergrowth of potassium feldspar and quartz are present in all San Diego County pegmatite-aplite dikes, principally in the hanging wall. Many of the potassium feldspar grains are wedge-shaped and flare toward the core. Comb-structure tourmaline, indicative of rapid growth (Lofgren 1980), is present at the country rock-pegmatite contact of the Himalaya dike (Fig. 3). Foord (1976) reports plumose and dendritic albite, as well as skeletal and elongated garnet in the hanging wall of the upper Himalaya dike.

In an effort to quantify crystallization parameters, we constrained mineral nucleation and growth rates to the cooling models. This necessitates rapid growth rates and variable nucleation rates for the main phase of magmatic crystallization. The simplest way to determine growth rates is to assume that crystallization began at the time of emplacement and continued until the solidus was reached. Thus, in the cooling models presented, the crystallization interval corresponds to the time it took the melts to cool from 650 to ~550 °C. This crystallization interval accounts for only the main phase of magmatic crystallization, with crystallization in the pockets continuing down to temperatures as low as ~425 °C (London 1986), and would not account for any subsolidus modifications. The assumption that crystal growth began at the time of emplacement will yield minimum growth rates, as the experimental work of Swanson (1977), Fenn (1977), and London et al. (1989) all demonstrate that there is a considerable nucleation lag time between when a haplogranitic melt has cooled through the liquidus and when crystallization actually begins. According to the experimental work of London et al. (1989), the greater the undercooling prior to the onset of crystallization, the more the resultant textures resemble pegmatites instead of granites. Additionally, London et al. (1989) found that mineral zoning patterns, sharp changes in grain size, mineral textures, and oriented fabrics that typify pegmatites could all be replicated experimentally from undercooling vapor-undersaturated Macusani glass.

We have no way of quantifying the lag time or the absolute degree of undercooling that occurred before nucleation and crystal growth began for the San Diego County pegmatite-aplite dikes. However, we can still make some minimum estimates of growth rates based on the cooling models. The lower 35 cm of the Mission dike consists of layered aplite, the top of which had cooled to 550 °C in about 5 d according to our model (Fig. 5c). Using a time constraint of 5 d suggests that, on the whole, the solidification rate for the layered aplite portion of the dike was ~7 cm/day or 8.1×10^{-5} cm/s, which would necessitate both high nucleation and growth rates for the millimeter-size aplite grains. The solidification rate for the 1 m wide Himalaya dike was ~20 cm/day, if crystallization was initiated upon emplacement and continued throughout the course of cooling from 650 to 550 °C in the 5 d period suggested by the cooling models (Fig. 5d). In the Himalaya dike some hanging wall potassium feldspar megacrysts and tourmaline crystals exceed 10 cm in length. If their growth occurred during half of the cooling time of the dike to 550 °C, then the crystals would have had growth rates of about 5×10^{-5} cm/s or about 4 cm/day.

These growth rates are much faster than those determined by Swanson (1977) and Fenn (1977) for potassium feldspar in haplogranitic melts of 10^{-6} – 10^{-7} cm/s.

To further evaluate crystallization dynamics in the pegmatite-aplite dikes, CSD studies were conducted for garnet crystals in the layered aplites. Garnet was chosen because it is abundant, euhedral, and nearly spherical in shape, thus facilitating more accurate determinations of grain volumes. CSD studies were not possible for the pegmatitic portions of the dikes because it would entail measurement of individual grains in outcrop; these grains are too large to be measured in thin section and the determination of crystal volumes would be far more complicated for these irregular, non-spherical grains. Therefore the CSD results apply strictly to the aplitic portion of the dikes. The nucleation densities, n^0 , were determined for garnet in the aplitic portions of the Himalaya, Mission, and George Ashley dikes, as previously discussed. To determine growth rate (*G*) or nucleation rate (*J*) from CSD, we must know one of these two variables to evaluate Equation 8.

Brandeis and Jaupart (1987a, 1987b) used dimensional analysis of crystallization equations for conductive cooling together with crystal size data from thin dikes to obtain values for nucleation rates and growth rates. Following kinetic theory, the rates for both variables can be expressed as a function of temperature and undercooling. Both nucleation and growth rate functions yield Gaussian curves with respect to degree of undercooling (Brandeis et al. 1984). In geologic systems, the total range of possible nucleation rates is much larger than that of growth rates. Brandeis and Jaupart (1987a, 1987b) suggested that local growth rates in silicate systems generally range from 10^{-10} to 10^{-8} cm/s, and local nucleation rates are on the order of 10^{-7} – 10^{-3} /cm³ s. Their data from dike margins constrain growth rates of close to 10^{-7} cm/s and nucleation rates of ~1/cm³ s, which correspond to a crystallization time of ~ 10^5 – 10^7 s for conductive cooling of dikes <10 m wide. Swanson (1977) experimentally determined growth rates of quartz, potassium feldspar, and plagioclase in undercooled (200 °C minimum) haplogranite with 3.5 wt% H₂O to be 10^{-6} – 10^{-8} cm/s. Nucleation densities for all three phases ranged from 10^7 – 10^8 sites/cm³. To estimate nucleation and growth parameters for the San Diego County pegmatite-aplite dikes that are consistent with the short times indicated by the cooling models, and the experimentally determined rates discussed above, we have chosen growth rates of 10^{-7} and 10^{-6} cm/s.

Following Cashman (1990) and Brandeis and Jaupart (1987a), the crystal growth time (τ) can be related to the growth rate (*G*) and nucleation rate (*J*) functions by:

$$= (G^3 J)^{\frac{1}{4}} \quad (10)$$

If a growth rate of 10^{-7} cm/s is used along with the n^0 value obtained from the garnet CSD study, then the nucleation rate *J*, determined from Equation 8, is equal to 1.9×10^{-1} , 6.37, and 5.54×10^{-1} /cm³ s for the George Ashley, Mission, and Himalaya dikes respectively. Substituting these determined nucleation rates into Equation 10 yield garnet crystal growth times (τ) of 2.69×10^5 s or about 3.1 days for the George Ashley dike, 1.11×10^5 s or about 1.3 days for the Mission dike, and 2.06×10^5 s or about 2.38 days for the Himalaya dike. A higher growth rate

of 10^{-6} cm/s yields garnet crystal growth times () of 2.69×10^4 s or about 0.31 days for the George Ashley dike, 1.11×10^4 s or about 0.13 days for the Mission dike, and 2.06×10^4 s or about 0.24 days for the Himalaya dike. If, as discussed previously, the entire 35 cm thick line rock portion of the Mission dike cooled to below 550°C in only 5 d, then garnet growth rates on the order of 10^{-7} cm/s yield growth times that are too long to be consistent with the cooling models. Faster growth rates of at least 10^{-6} cm/s are required to be consistent with the short cooling times.

Thus, the implication of constraining mineral growth rates to the cooling models is that crystals of garnet and other minerals in the aplites (quartz, albite, muscovite, and tourmaline) grew in only a few hours. Additionally, the largest crystals in the hanging wall of the pegmatite-aplite dikes required only a day or so to grow. Varying initial parameters, such as using a higher country rock temperature, will of course slow down cooling rates and thus mineral growth rates. However, the rates do not change by orders of magnitude. For example, the Himalaya dike cools to below 450°C in <30 d even if it is emplaced into hotter country rock of 300°C instead of 150°C . The parameter that does vary throughout crystallization of the dikes is nucleation rate. If growth rates are uniformly high at 10^{-6} cm/s or faster, then nucleation rates must be higher during crystallization of the aplitic portion than the pegmatitic portion of the dikes.

DISCUSSION

Reconstructing the crystallization history of the San Diego County pegmatite-aplite dikes involves interpreting the textures preserved in the dikes in the context of the constraints placed on the system by rapid cooling. Each pegmatite-aplite dike has its own unique characteristics and therefore each dike has a somewhat different crystallization history. We focus our subsequent discussion on the Himalaya and George Ashley dikes because they display between them various features common to many pegmatite-aplite dikes.

Textural and structural features allow these dikes to be subdivided into three generalized zones: a footwall aplite, a core and pocket zone, and a massive and graphic pegmatite hanging wall (Fig. 4). The footwall aplite can be subdivided further into a basal, non-layered albite-aplite and an upper layered aplite. In the George Ashley and Himalaya dikes, the boundary between the two is marked by a distinct garnet layer (with minor tourmaline) and garnet-rich layers occur throughout the layered aplite zone. The "main garnet layer" in the lower Himalaya dike (Fig. 4) can be traced for almost 1000 m. Tapered crystals of potassium feldspar are oriented perpendicular to the layers and enlarge toward the center of the dike. The core zone is enriched in quartz and contains miarolitic pockets that host various minerals including tourmaline, quartz, garnet, micas, and feldspars. The hanging wall is characterized by an abundance of wedge-shaped, perthitic potassium feldspar crystals that enlarge downward toward the core zone. These potassium feldspar crystals form graphic intergrowths with quartz in the upper portions of the hanging wall, but form separate phases as the core zone is approached in both the George Ashley and Himalaya dikes. Foord (1976) suggested that so-

lidification of the graphic pegmatite in the hanging wall of the lower Himalaya dike began after a significant portion of the basal non-layered aplite had formed, and thus crystallized at the same time as the layered aplite above the "main garnet layer." This conclusion was substantiated by stable isotope systematics and fluid inclusion studies of Taylor et al. (1979) who suggested that, prior to solidification of the pegmatite along the upper contact, the dike behaved as an open system with aqueous fluids lost primarily to overlying wall rocks. Foord (1976) suggested that the comb structure tourmaline at the pegmatite-country rock contact in the upper Himalaya dike (Fig. 3) resulted from the interaction of B from the Himalaya melt with Fe and Mg in the country rock.

The crystallization history of the dikes begins subsequent to emplacement and undercooling with albite and quartz the first phases to crystallize in the footwall. This is consistent with the sequence of phases that crystallized from undercooled H_2O -undersaturated Macusani glass documented by London et al. (1989) (i.e., albite and quartz followed by potassium feldspar). In the undercooling region that maximizes growth rates for albite, quartz, and potassium feldspar, the nucleation densities of albite and quartz are higher than those of potassium feldspar (Fenn 1977; Swanson and Fenn 1986; London et al. 1989). This difference results in many small crystals of albite and quartz and the occasional tapered megacrysts of potassium feldspar that flare toward the pegmatite center. As the melt is undersaturated with respect to H_2O and other volatiles, the initial phases precipitating are anhydrous, which leads to the enrichment of excluded components such as H_2O , B, Li, K, Fe, and Mn, in the residual melt. The rapid crystallization of the melt leads very quickly to an inhomogeneous upward distribution of volatiles. When the hanging wall begins to crystallize, there is already a sizable thickness of albite-aplite and thus the boundary layers at the top and bottom of the dike will not have the same composition. The rapid nucleation and growth of albite

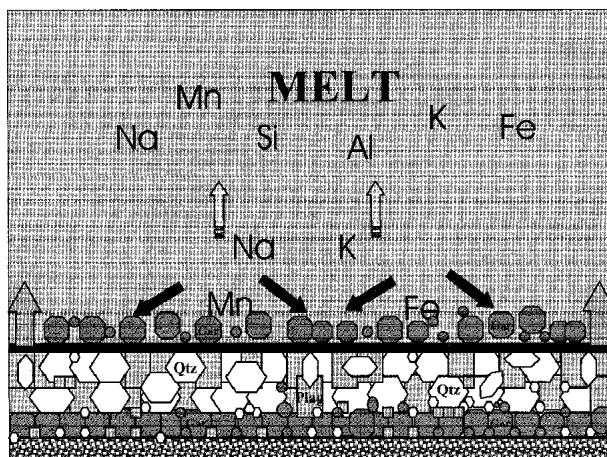


FIGURE 8. Crystallization of garnet at the boundary layer during the formation of line rock. Mn and Fe diffuse to the growing crystals whereas excluded components such as Na, K, and volatiles diffuse away from the crystallization front. Crystallization of garnet continues until the boundary layer is depleted in Mn and Fe at which time phases such as quartz and albite nucleate and grow.

and quartz with minor muscovite and potassium feldspar would result in the development of a boundary layer of excluded components (initially Mn and Fe) ahead of the crystallization front that would accumulate to the point of local saturation and thus set up the right conditions for oscillatory crystallization to begin (Fig. 8). The saturation of Mn and Fe at the crystallization front led to the nucleation and growth of garnet with minor amounts of tourmaline, which continued until the concentration of Mn and Fe decreased. The nucleation and growth of garnet would then slow dramatically until the concentration of the excluded elements built up again to saturation levels. During line rock formation, concentrations of B were not sufficiently high to permit the crystallization of more than minor amounts of tourmaline. Albite and quartz nucleation and growth continued throughout. The upward concentration of volatiles, particularly B, is demonstrated by the presence of comb structure tourmaline at the pegmatite-country rock contact in the upper Himalaya dike. The presence of tourmaline at the contact suggests an unequal distribution of B in the melt at the time crystallization occurred in the hanging wall. Tourmaline is rare in the footwall portions of both the George Ashley and lower Himalaya dikes until you get close to the pocket zone. Foord (1976) described three tourmaline layers that occur at the top of the layered aplite in the lower Himalaya dike just below the pocket zone. The increase in volatiles in the hanging wall would decrease the potassium feldspar nucleation rate but not the growth rate, allowing for fewer, but larger potassium feldspar crystals to grow (Fenn 1977; London 1992). The fact that potassium feldspar forms graphic intergrowths with quartz attests to the continued strong undercooling and rapid crystallization from a volatile enriched but still undersaturated melt (Fenn 1986). As crystallization proceeds toward the core and the volatiles continue to accumulate, graphic intergrowths of potassium feldspar and quartz cease to form, giving way to crystallization of separate crystals of each.

The George Ashley dike differs from the Himalaya and Mission dikes in that the layered aplite occurs well above the base of the dike. Upon emplacement of this dike, nucleation and crystallization took place along both dike margins, which resulted in the development of granular pegmatite. There is an abrupt change in the footwall from the granular pegmatite into the aplite suggesting that the kinetics of crystallization changed dramatically. Webber et al. (1997) suggested that there was an abrupt increase in the nucleation rate coincident with the onset of line rock formation. We believe that the trigger for the destabilization of the system, which initiated the crystallization of fine-grained materials, was a sudden pressure loss within the dike caused either by dike rupture or the dilatancy of the dike due to fracture propagation of the stressed country rock. Thus, in the George Ashley dike, it appears that a sudden drop in pressure, not a loss of volatiles as proposed by Jahns and Tuttle (1963), was the trigger for strong undercooling and disequilibrium oscillatory crystallization. We favor dike dilatancy as a mechanism for the pressure reduction. Line rock formation would cease when sufficient volatile phases had accumulated and the degree of undercooling decreased. Normal equilibrium granular crystallization would then resume. We believe that oscillatory nucleation and crystallization can be initiated

by high degrees of undercooling alone or by an external forcing factor such as pressure reduction produced by dike dilatancy (fracture propagation). Any event that results in strong undercooling has the potential to initiate line rock formation. Emplacement of melt into relatively cool country rocks, loss of volatiles to the country rock, crystallization of tourmaline that effectively removes boron from the melt (Rockhold et al. 1987), and dike rupture or dike dilatancy, all can increase the degree of undercooling of the melt and act as a trigger to destabilize the crystallization dynamics of the pegmatite system. Such events potentially can initiate rapid heterogeneous nucleation and oscillatory crystal growth, the development of a layer of excluded components in front of the crystallization front, and the formation of line rock.

Thus, the textures that characterize San Diego County pegmatite-aplite dikes are consistent with rapid growth rates for most of the cooling history of the dike, which were probably on the order of at least 10^{-5} – 10^{-6} cm/s. Nucleation rates were higher during crystallization of the relatively volatile-poor, fine-grained aplitic footwall than they were during crystallization of the more volatile-enriched, coarser-grained hanging walls. Rapid crystallization is consistent with the conductive cooling models for the thin, shallow, pegmatite-aplite dikes in San Diego County, which suggest the dikes cool in days to years.

ACKNOWLEDGMENTS

Helpful reviews were provided by Anthony D. Fowler, David London, George B. Morgan VI, and Jim Nizamoff and are gratefully acknowledged.

REFERENCES CITED

- Baker, D.R. (1996) Granitic melt viscosities: empirical and configurational entropy models for their calculation. *American Mineralogist*, 81, 126–134.
- Brandeis, G. and Jaupart, C. (1987a) Crystal sizes in intrusions of different sizes: Constraints on the cooling regime and the crystallization kinetics. In B.O. Mysen, Ed., *Magmatic Processes: Physicochemical Principles*, p. 307–318. The Geochemical Society, Pennsylvania State University, Pennsylvania.
- (1987b) The kinetics of nucleation and crystal growth and scaling laws for magmatic crystallization. *Contributions to Mineralogy and Petrology*, 96, 24–34.
- Brandeis, G., Jaupart, C., and Allegre, C.J. (1984) Nucleation, crystal growth and the thermal regime of cooling magmas. *Journal of Geophysical Research*, 89, 10161–10177.
- Cashman, K.V. (1990) Textural constraints on the kinetics of crystallization of igneous rocks. In *Mineralogical Society of America Reviews in Mineralogy*, 24, 259–314.
- Cashman, K.V. and Marsh, B.D. (1988) Crystal size distribution (CSD) in rocks and the kinetics and dynamics of crystallization II. Makaopuhi lava lake. *Contributions to Mineralogy and Petrology*, 99, 292–305.
- Fenn, P.M. (1977) The Nucleation and growth of alkali feldspars from hydrous melts. *The Canadian Mineralogist*, 15, 135–161.
- (1986) On the origin of graphic granite. *American Mineralogist*, 71, 325–330.
- Fisher, J., Foord, E.E., and Bricker, G.A. (1998) The geology, mineralogy, and history of the Himalaya Mine, Mesa Grande, San Diego County, California. *Rocks and Minerals*, 156–180.
- Foord, E.E. (1976) Mineralogy and petrogenesis of layered pegmatite-aplite dikes in the Mesa Grande District, San Diego County, California, 326 p. Ph.D. dissertation, Stanford University, California.
- (1977) The Himalaya dike system. *The Mineralogical Record*, 8, 461–474.
- Foord, E.E., Starkey, H.C., and Taggart, J.E., Jr. (1986) Mineralogy and paragenesis of “pocket clays” and associated minerals in complex granitic pegmatites, San Diego County, California. *American Mineralogist*, 71, 428–439.
- Foord, E.E., London, D., Kampf, A.R., Shigley, J.E., and Snee, L.W. (1991) Gem-bearing pegmatites of San Diego County, California. In M.J. Walawender and B.B. Hanan, Eds., *Geological Excursions in Southern California and Mexico*, Guidebook for the 1991 Annual Meeting, Geological Society of America, p. 3563–3592. San Diego State University, California.
- Huang, W.L. and Wyllie, P.J. (1981) Phase relationships of S-type granite with H₂O to 35 kbar: muscovite granite from Harney Peak, South Dakota. *Journal of Geophysical Research*, 86, 10515–10529.
- Jaeger, J.C. (1968) Cooling and solidification of igneous rocks. In H.H. Hess and A. Poldervaart, Eds., *Basalts, The Poldervaart Treatise on Rocks of Basaltic Com-*

- position, p. 503–537. Wiley, New York.
- Jahns, R.H. (1979) Gem-bearing pegmatites in San Diego County, California: The Stewart Mine, Pala district and the Himalaya Mine, Mesa Grande district. In P.L. Abbott and V.R. Todd, Eds., *Mesozoic Crystalline Rocks*, p. 3–38. San Diego State University, Department of Geological Sciences, California.
- Jahns, R.H. and Tuttle, O.F. (1963) Layered pegmatite-aplite intrusives. *Mineralogical Society of America Special Paper*, 1, 78–92.
- Jahns, R.H. and Wright, L.A. (1951) Gem- and lithium-bearing pegmatites of the Pala District, San Diego County, California. *California Division of Mines Special Report*, 7–A, 72 p.
- Kirkpatrick, R.J. (1977) Nucleation and growth of plagioclase, Makaopuhi and Alae lava lakes, Kilauea Volcano, Hawaii. *Geological Society of America Bulletin*, 88, 78–84.
- Kleck, W. (1996) Crystal settling in pegmatite magma. Abstracts and Program. Geological Association of Canada and Mineralogical Association of Canada, A–50.
- Lofgren, G. (1980) Experimental studies on the dynamic crystallization of silicate melts. In R.B. Hargraves, Ed., *Physics of Magmatic Processes*, p. 487–551. Princeton University Press, New Jersey.
- London, D. (1986) Formation of tourmaline-rich gem pockets in miarolitic pegmatites. *American Mineralogist*, 71, 396–405.
- (1992) The application of experimental petrology to the genesis and crystallization of granitic pegmatites. *The Canadian Mineralogist*, 30, 499–540.
- London, D., Morgan, G.B., and Hervig, R.L. (1989) Vapor-undersaturated experiments with Macusani glass + H₂O at 200 MPa, and the internal differentiation of granitic pegmatites. *Contributions to Mineralogy and Petrology*, 102, 1–17.
- MacLellan, H.E. and Trembath, L.T. (1991) The role of quartz crystallization in the development and preservation of igneous texture in granitic rocks: Experimental evidence at 1 kbar. *American Mineralogist*, 76, 1291–1305.
- Marsh, B.D. (1988) Crystal size distribution (CSD) in rocks and the kinetics and dynamics of crystallization I. Theory. *Contributions to Mineralogy and Petrology*, 99, 277–291.
- McBirney, A.R. (1993) *Igneous Petrology*, 508 p. Jones and Bartlett, Boston.
- Philpotts, A.R. (1990) *Principles of Igneous and Metamorphic Petrology*, 498 p. Prentice Hall, New Jersey.
- Randolph, A.D. and Larson, M.A. (1971) *Theory of particulate processes*, New York, Academic Press, 251p.
- Rockhold, J.R., Nabelek, P.I., and Glascock, M.D. (1987) Origin of rhythmic layering in the Calamity Peak satellite pluton of the Harney Peak Granite, South Dakota: The role of boron. *Geochemica et Cosmochimica Acta*, 51, 487–496.
- Snee, L.W. and Foord, E.E. (1991) ⁴⁰Ar/³⁹Ar thermochronology of granitic pegmatites and host rocks, San Diego County, California. *Geological Society of America Abstracts with Programs*, San Diego, California, 23, 189.
- Swanson, S.E. (1977) Relation of nucleation and crystal-growth rate to the development of granitic textures. *American Mineralogist*, 62, 966–978.
- Swanson, S.E. and Fenn, P.M. (1986) Quartz crystallization in igneous rocks. *American Mineralogist*, 71, 331–342.
- Taylor, B.E., Foord, E.E., and Friedrichsen, H. (1979) Stable isotope and fluid inclusion studies of gem-bearing granitic pegmatite-aplite dikes, San Diego Co., California. *Contributions to Mineralogy and Petrology*, 68, 187–205.
- Wager, L.R. (1961) A note on the origin of ophitic texture in the chilled olivine gabbro of the Skaergaard intrusion. *Geological Magazine*, 98, 353–366.
- Webber, K.L., Falster, A.U., Simmons, Wm.B., and Foord, E.E. (1997) The role of diffusion-controlled oscillatory nucleation in the formation of line rock in pegmatite-aplite dikes. *Journal of Petrology*, 38, 1777–1791.

MANUSCRIPT RECEIVED SEPTEMBER 15, 1998

MANUSCRIPT ACCEPTED DECEMBER 2, 1998

PAPER HANDLED BY DAVID LONDON